This article has been accepted for publication in a future issue of this journal, but has not been fully edited. Content may change prior to final publication. Citation information: DOI 10.1109/TMECH.2017.2765081, IEEE/ASME Transactions on Mechatronics

A Cable Driven Flexible Robotic Grasper with Lego-like Modular and Reconfigurable Joints

Changsheng Li, Xiaoyi Gu, *Student Member, IEEE*, Hongliang Ren*, *Senior Member, IEEE*

***Abstract*—This paper proposes a Modular and Reconfigurable Cable-driven robotic grasper (MoReCa Grasper) for grasping diverse unknown objects in unstructured environments, which integrates the characteristics of full actuation and under-actuation. The mechanical design of this robotic grasper is introduced with a focus on its Lego-like modular design feature and reconfigurable flexible joints. With these features, the length of this robotic grasper can be arbitrarily changed through the addition or removal of the Lego-like finger modules connected by magnets without rerouting or breaking the cables. The shape and degree of freedom (DOF) of the robotic grasper can be adjusted by changing the states of the joints using embedded clutches. When the joints are locked, the grasper can maintain its shape without additional power from actuators leading to better energy efficiency. The kinematics, workspace, and contact force are analyzed. On this basis, an automatically reshaping method (ARM) based on the motor's current during the operation is proposed. Lastly, an example prototype of the robotic grasper with two fingers (four modules each), is built and tested. In the first experiment, the maximum grasping force is obtained. The second experiment demonstrates the ability of grasping diverse objects via changing the number of the modules and presetting the shape of the robotic grasper. The effectiveness of the ARM is verified in the third experiment.**

***Index Terms*—Robotic grasper, modular construction, cable driven, reconfigurable joint, Lego-like**

I. Introduction

Performing grasping tasks in unstructured environments is challenging because the object properties are often unknown [1], especially when the shapes of the objects are diverse, such as long, small, soft, and complex. These tasks are often essential and meaningful for the wide application ranging from industrial production, space and ocean system, to daily life. The degree of difficulty will significantly increase when a single robotic grasper is required to perform a wide range of grasping motions.

To achieve the grasping motion in unstructured environments, a full actuation mechanism has been widely accepted in the design of various robotic graspers. These graspers are capable of achieving high kinematic accuracy by actively controlling every joint. However, complex mechanical structures and high manufacturing cost restrict the promotion of this kind of graspers. Moreover, the effective grasping of unknown objects using this grasping relies heavily on simulating the geometry of the object beforehand [2, 3]. The exact model of the objects is difficult to build since most of the shapes of the objects are usually irregular and complex, and the relationship between the objects and the environments are uncertain. This makes it difficult to grasp unknown objects successfully. Even so, researchers have developed various robotic graspers/hands. The Stanford/JPL hand [4], used for industrial purposes, has three fingers with three degrees of freedom (DOFs) each. The Utah/MIT hand [5] has four fingers with four DOFs each, in which the actuation system is removed from the body of the hand and tendons are routed to the base of the manipulator. Another representative is the DLR hand [6]. It has four identical fingers with four joints, and one additional DOF in the palm. Although these hands are like human hands and highly flexible, complex motion planning is needed to grasp different objects.

The development of the under-actuation mechanism paves a new way for designing robotic graspers, which are able to perform grasping of various objects with simplified mechanical structures, sensing and control systems [7-11] (e.g., the TBM hand [10], the SSL hand [11] and the SDM hand [7]). The coupled and redundant DOFs make these hands adaptable to the geometry of the objects through intrinsic compliance, increasing the contact points and minimize contact forces [12, 13]. In addition, underactuated hands have some advantages such as low cost, simple design and fabrication [14]. However, for light objects, the benefits of the underactuated hands are degraded because the coupled joints are difficult to be constrained by the geometry of the objects. The objects may even be dislodged or damaged in the grasp acquisition process for light weight objects or redundant contact forces [15]. Another disadvantage of the underactuated hands is the lack of dexterity. The pose of each finger is hard to be accurately pre-designed. Accordingly, some ingenious designs have been applied to improve the performance: e.g. a brake is used to realize high braking force [16] and a selectively compliant underactuated hand is designed to grasp a broad spectrum of objects [17].

Design and analysis of transmission systems in robotic hands/graspers have also been addressed in the past decade

* Correspondence to Hongliang Ren (ren@nus.edu.sg).

This work is supported by Singapore Millennium Foundation under Grant R-397-000-201-592 and Office of Naval Research Global under grant ONRG-NICOP-N62909-15-1-2029 awarded to Dr. Hongliang Ren.

Changsheng Li, Xiaoyi Gu and Hongliang Ren are with the Department of Biomedical Engineering, National University of Singapore, Singapore 117575, Singapore. (e-mail: lics32@163.com, xiaoyi900217@gmail.com, ren@nus.edu.sg)

1083-4435 (c) 2017 IEEE. Personal use is permitted, but republication/redistribution requires IEEE permission. See http://www.ieee.org/publications_standards/publications/rights/index.html for more information.

This article has been accepted for publication in a future issue of this journal, but has not been fully edited. Content may change prior to final publication. Citation information: DOI 10.1109/TMECH.2017.2765081, IEEE/ASME Transactions on Mechatronics

[18-20]. Bar linkage and direct-driven mode [21-23] have effectively improved the control performance because of the rigid connection [24]. However, the power is usually not enough for a dynamic manipulation or heavier objects because the working volume of the actuator is limited [25]. The cable-driven mode has been widely used in robotic hand/grasper designs, allowing to place actuators far away from the main body [26, 27]. The hands/graspers with versatile grasping patterns, minimal volume and weights have better compatibilities with other robotic systems.

From the above analysis, we conclude that it is still a challenge to develop a versatile robotic hand/grasper for grasping diverse objects in unstructured environment. For existing designs, complex control, mechanisms or sensors are necessary for effective grasping. One important reason is that the size, workspace and the grasp shape of the current robotic hand/grasper are unchangeable once designed. If we could break through these concepts and develop a robotic hand/grasper with variable size and shape, there would be a better grasping performance.

In this paper, we propose a cable driven robotic grasper with modular, reconfigurable flexible joints that possesses the merits of low cost, simple control and fabrication, and more importantly, effectiveness of grasping objects with diverse sizes, shapes and textures.

The primary contributions of our work are summarized as follows:

- A new framework of Lego-like modular mechanism is proposed for the first time, to the best of our knowledge, for developing cable-driven robotic graspers. The size, workspace and number of the robotic grasper's fingers can be changed by the modular mechanism.
- The joints of the robotic hand are reconfigurable, thus the shape/workspace of the robotic hand can be set online and the DOFs are changeable.

The rest of this paper is organized as follows. Section II describes the design of the robotic grasper. In Section III, the characteristics of this robotic grasper are discussed, followed by kinematics, workspace and force analysis in Section IV. In Section V, two experiments are presented. One experiment demonstrates the superiority of the proposed robotic grasper on grasping diverse objects, and the other experiment verifies the feasibility of the Automatically Reshaping Method (ARM). Finally, these results are analyzed and ideas for future work are presented.

II. Mechanical Design

A. System overview

The design objective is to grasp diverse daily necessities through combining simple Lego-like modular mechanisms, sensors, control techniques, and low-cost processing methods. In this design, the robotic grasper has two or more fingers, and each finger has several removable modules based on the Lego-like interlocking modular design concept. The number of fingers and modules can be easily adjusted when grasping diverse objects. The fingers are driven by DC motors via Bowden-cables. Each finger has four finger modules, which are connected through magnets. Each finger module includes a reconfigurable joint that can be locked or unlocked by a clutch.

B. Finger design

As mentioned above, the MoReCa robotic grasper introduce the design concept of modularization to cable-driven multi-segment manipulators. The number of modules can be increased to improve the reliability of grasping longer or complex shaped objects. The number can also be reduced to make the action more straightforward and easy to achieve when grasping smaller objects.

1) Finger module design and connection

The key design issue is to develop finger modules that can be installed or removed quickly and manually from the finger without any additional tools. For this purpose, the difficulty lies in how to connect each finger module. We were inspired by Lego and found that direct connection with magnets and gender design is the best way.

The details of the finger module are shown in Fig. 1. The magnets assembled on the two ends of the modules are designed to connect the adjacent modules. Gender design with one male side and one female side is adopted to enhance connection strength.

In the state of grasping objects, the contact surfaces of the modules are under pressure because of the reaction force of the object and the active force of driving system, thus, there is no direct relationship between the grasping force and the magnet attraction. Ordinary magnets can satisfy our requirements, because the magnets only need to provide an attraction to support the self-weight of the robotic grasper in a no-load state. In this design, we choose NdFeB magnets with the size of $5\ \text{mm} \times 10\ \text{mm} \times 20\ \text{mm}$ each. Compared with other connecting mechanisms based on mechanical locks, this mode makes it more convenient to install or remove the modules without any extra operation

We use a cable-driven method to actuate the fingers and multiple cables run through all the finger modules. Hence, another important feature and design challenge is how to deal with the cables when installing or removing the finger modules from the robotic grasper, either before (offline) or during (online) the operation. The solution is the staggered deep grooves in the sides of the modules. In that way, the cables are forced to cross through them and prevents the cable from rolling out of grooves.

2) Reconfigurable Joints

When the length of the robotic grasper is determined, increasing the contact area with the objects is an effective method to improve grasping performance. There are two approaches to increase the contact area. One is to make the robotic grasper compliant to objects and the other is to make the shape of the robotic grasper be the same as the objects. The grasping ability can be greatly improved if these two approaches can be combined, which is almost impossible with existing designs. We propose clutch based reconfigurable joints aiming to solve it.

1083-4435 (c) 2017 IEEE. Personal use is permitted, but republication/redistribution requires IEEE permission. See http://www.ieee.org/publications_standards/publications/rights/index.html for more information.

This article has been accepted for publication in a future issue of this journal, but has not been fully edited. Content may change prior to final publication. Citation information: DOI 10.1109/TMECH.2017.2765081, IEEE/ASME Transactions on Mechatronics

As shown in Fig. 1 (c), each finger module has one joint with one DOF. The clutches are installed to connect the joint. When the clutch is locked, the joint is locked, and when the clutch is unlocked, the joint is active. The DOF of the robotic grasper can also be changed by locking or unlocking the clutches, which means that when the number of the DOF is one, the robotic grasper is fully actuated or else the grasper is underactuated. In order to form different shapes for the robotic hand, the clutches can be unlocked first, and then the clutches are controlled to be locked when the joints are rotated to a certain angle.

In addition, there is another benefit for this kind of reconfigurable joint. If all the joints are locked when grasping, the locked joints allow the robotic grasper to remain in a fixed state to minimize the continuous current of motors and thus improve the lifespan of the motors.

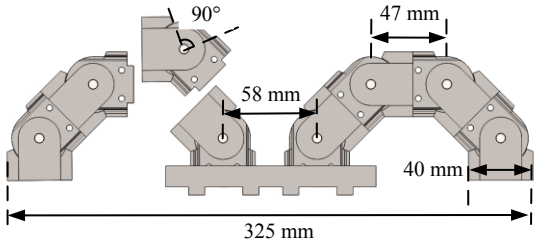

(a)

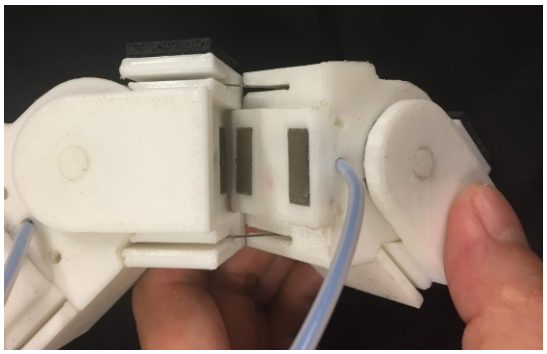

(b)

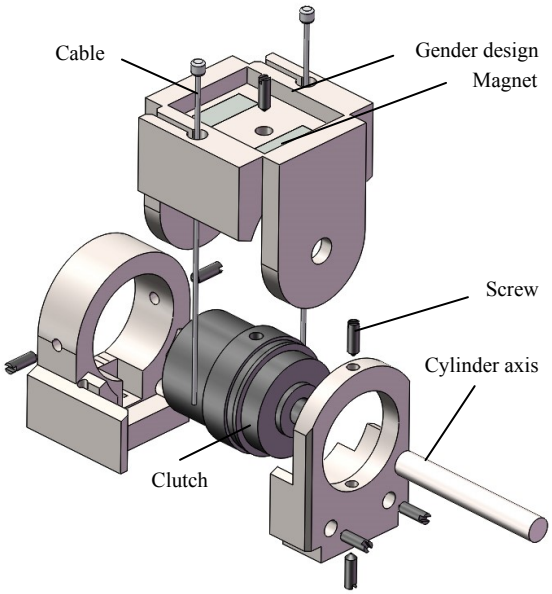

(c)

Fig. 1. The robotic grasper: (a) Schematic of the robotic grasper; (b) The design of the finger module junction; (c) Details of the finger module

3) Actuators

Actuators adopted in this design are DC motors, each connected to a back-drivable tendon spool. This tendon spool is allowed to be rotated passively to change the length of the cable when installing and removing the finger module. For each finger, two Bowden-cables are used to keep the driving system further away from the robotic grasper, thus reducing the volume and weight of the robotic grasper and expanding its operation range. One of them connects the finger modules and tendon spool. The other connects the finger modules and spring. The spring provides pulling force to recover the finger position to initial state. The motion of the fingers is driven by the cables when the tendon spools rotate.

4) Sensor

Another feature of this robotic grasper is the sensor. In order to change the shape of the robotic grasper when grasping objects, the contact force between the robotic grasper and the object needs to be detected. The common method is to install multiple force sensors in each finger module, which may increase complexity and reduce reliability. Thus, the motor current sensor instead of the force sensor is adopted in this design to detect the force of each modular. Due to the joint friction and the noise of current, the measuring accuracy of this method is not extremely high but enough for the general grasping.

III. Analysis on the Robotic Grasper

A. Kinematics Analysis

The purpose of kinematics analysis is to establish the relationship between the pose of the robotic grasper and the length variation of the cable for control. As shown in Fig. 2, $O_G - X_G Y_G Z_G$ is defined as the global coordinate, $O_i - X_i Y_i Z_i (i = 1,2,\cdots,n)$ is defined as the local coordinates on corresponding joints. The length variation of the cable and the spring in each joint are defined as $\Delta L_{c,i}$ and $\Delta L_{s,i}$, and the total length variation is defined as ΔL_c , and ΔL_s. d represents the distance between the groove for the cable or spring and the axis of the module, θ_0 represents the initial angle when the robotic grasper is placed in vertical direction. In this design, $\theta_0 = 45°$. $\theta_i \in (-45°, +45°)$ represents the angle of rotation of the i-th finger segment module. The relationship between $\Delta L_{c,i}$, $\Delta L_{s,i}$ and θ_i can be described by:

$$\begin{cases} \Delta L_{c,\mathrm{i}} = 2d\left(tan\theta_0 - \dfrac{\sin\left(\theta_0 - \frac{\theta_i}{2}\right)}{\cos\theta_0}\right) \\ \Delta L_{s,\mathrm{i}} = 2d\left(tan\theta_0 - \dfrac{\sin\left(\theta_0 + \frac{\theta_i}{2}\right)}{\cos\theta_0}\right) \end{cases} \quad (1)$$

Then,

$$\begin{cases} \Delta L_c = \sum_{i=1}^{n} \Delta L_{c,i} \\ \Delta L_s = \sum_{i=1}^{n} \Delta L_{s,i} \end{cases} \quad (2)$$

1083-4435 (c) 2017 IEEE. Personal use is permitted, but republication/redistribution requires IEEE permission. See http://www.ieee.org/publications_standards/publications/rights/index.html for more information.

This article has been accepted for publication in a future issue of this journal, but has not been fully edited. Content may change prior to final publication. Citation information: DOI 10.1109/TMECH.2017.2765081, IEEE/ASME Transactions on Mechatronics

$P_i = [-d \quad 0 \quad 0 \quad 1]$ represents the terminal point of the i th finger module, which is at the end of each finger module. The coordinate transformation matrix can be described as:

$$
{}^{i-1}_{i}T = \begin{cases} \begin{bmatrix} \cos(\theta_i) & -\sin(\theta_i) & 0 & -H\sin(\theta_i) \\ \sin(\theta_i) & \cos(\theta_i) & 0 & H\cos(\theta_i) \\ 0 & 0 & 1 & 0 \\ 0 & 0 & 0 & 1 \end{bmatrix}, i = 1,2,\cdots,n-1 \\ \begin{bmatrix} \cos(\theta_i) & -\sin(\theta_i) & 0 & \frac{-H\sin(\theta_i)}{2} \\ \sin(\theta_i) & \cos(\theta_i) & 0 & \frac{-H\cos(\theta_i)}{2} \\ 0 & 0 & 1 & 0 \\ 0 & 0 & 0 & 1 \end{bmatrix}, i = n \end{cases} \tag{3}
$$

P_n can be described in the base coordinate by:

$$P_n = \prod_{i=1}^{n} {}^{i-1}_{i}T \, {}^{n}P_n \tag{4}$$

The relationship between ΔL_c and P_n can be obtained by solving (4).

The number of active joints can be defined as N_{act}. When $N_{act} = 1$, the DOF of the robotic grasper is one, and the kinematic solution can be determined. When $N_{act} > 1$, the kinematic solution is uncertain.

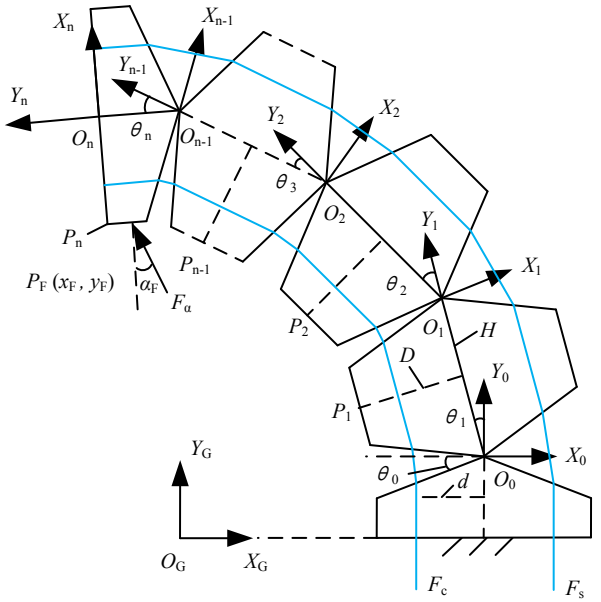

Fig. 2. Kinematics analysis of one finger (The dashed lines of P_{n-1} represent the omitted modules)

B. Workspace Analysis

This section analyzes the grasping range of the robotic grasper with two modular fingers and possible factors that influence the workspace. Due to the modular design, the analysis here can be extended to multi-modular fingers. As shown in Fig. 2, points P_i on the finger modules are taken as contact points for workspace analysis. Every finger module has the possibility to contact the object during the grasping process. The workspace is analyzed via MATLAB. θ_i is taken as input variables with a proper step size in the range from $-45°$ to $45°$. P_i are calculated based on the results of (4).

Fig. 3 shows the workspaces of 3 typical states of the robotic grasper, which are the areas P_i can reach. For the first state, there are 3 joints in each finger. All the joints are unlocked which is suitable for grasping irregular and large objects (Fig. 3 (a)). For the second state, there are 4 joints in each finger. The first joint is unlocked and other joints are locked in 0°, which is suitable for grasping long and soft objects (Fig. 3 (b)). For the third state, there are 2 joints in each finger. The first joint is locked in 0°, and the second joint is released. This kind of shape with a less active joint is suitable to grasp small and light objects (Fig. 3 (c)).

According to simulation results, the states of the joints and the number of the finger modules determine the workspace. The reachable areas of the points P_i in the first state, with 3 DOFs each finger (Fig. 3(a)) are denser than those in the second and third states, with 1 DOF each finger (Fig. 3(b)-(c)), thus the more unlocked joints, the higher possibility of contacting with objects. Another aspect, the reachable range of the points P_i in the second state, with 4 finger modules each finger (Fig. 3(b)), is larger than those in the first and third states, with 3 and 1 finger modules each finger (Fig. 3(a) and (c)), which indicates that more modules provide larger grasping space.

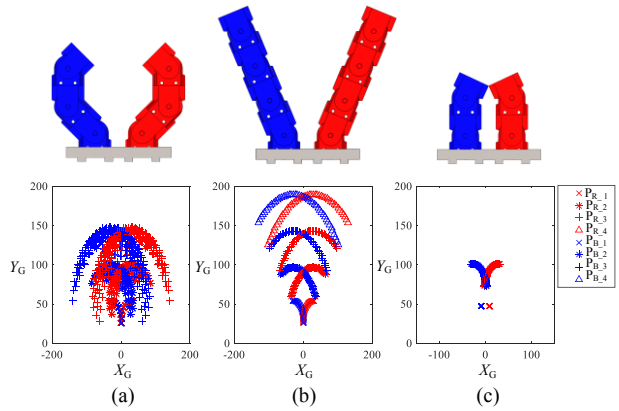

Fig. 3. Three typical states of the robotic grasper and the corresponding workspace. P_{B_1} - P_{B_4} represent the terminal points of the blue finger, and P_{R_1}-P_{R_4} represent the terminal points of the red finger.

C. Contact Force Analysis

The detection of contact force is used for controlling the shape of the robotic grasper. High-precision measurement is not required, so the rough force analysis is given. The grasping process is slow and the weight of the robotic grasper is far below the grasping force. To simplify the analysis, the influence of gravity, friction and other secondary factors are ignored. As shown in Fig. 2, we define $\alpha_F \in (-90°, +90°)$ and $P_F(x_F, y_F)$ as incident angle and point of action of the force F_a acting on the n-th finger modular respectively. P_F can be calculated through the kinematic solution of the robotic grasper.

F_c is the pulling force of the cable. Based on the moment balance principle, Equation (6) can be obtained:

$$(F_c - F_s)d - F_a[\cos(\textstyle\sum_{i=1}^{n}\theta_i + \alpha_F)\, y_F + \sin(\sum_{i=1}^{n}\theta_i + \alpha_F)x_F] = 0 \tag{6}$$

F_s can be described by:

1083-4435 (c) 2017 IEEE. Personal use is permitted, but republication/redistribution requires IEEE permission. See http://www.ieee.org/publications_standards/publications/rights/index.html for more information.

This article has been accepted for publication in a future issue of this journal, but has not been fully edited. Content may change prior to final publication. Citation information: DOI 10.1109/TMECH.2017.2765081, IEEE/ASME Transactions on Mechatronics

$$F_s = k_s \Delta L_s \quad (7)$$

where k_s is the spring coefficient.

I_m is defined as the current of the motor. The relationship between F_c and I_m can be regarded as a linear relation and can be described by:

$$F_c = k_c I_m \quad (8)$$

where k_c is the proportionality coefficient.

Combining (6)-(8), we can obtain the relationship between F_a and I_m.

$$F_a = \frac{(k_c I_m - k_s \Delta L_s) d}{\cos(\sum_{i=1}^{n} \theta_i + \alpha_F) y_F + \sin(\sum_{i=1}^{n} \theta_i + \alpha_F) x_F} \quad (9)$$

(9) indicates that there is a positive correlation between F_a and I_m when the shape of the robotic grasper is determined.

IV. Automatically Reshaping Method

One of the distinct features of this robotic grasper is reconfigurable joints, which means the shape of the robotic grasper can be changed when grasping diverse objects. If the shape of the robot grasper is more conformable to the object, the contact area will be larger and the grasping effect will be better. There are mainly two methods to change the shape of the robotic grasper.

The first is the presetting shape method. The shape of the robotic grasper is preset before grasping, which is easy to be achieved. As a result, we focus on the second method: ARM during the grasping process. The main idea of ARM is reshaping the robotic grasper by changing the states of the joints based on the contact force, which is taken as a trigger signal to determine if the robotic grasper contacts the object.

As shown in Fig. 4, we take one finger with four finger modules as an example to demonstrate the proposed reshaping method in handling a complex concave object. Firstly, the robotic grasper is set to its initial state, in which the open angle of the robotic grasper is the largest due to the tension of the spring. The first joint which is the nearest to the base is released while other joints are locked (Fig. 4 (a)). And then the first joint is rotated for grasping. When the contact force of the first module is detected, the second joint is unlocked and the other joints are locked (Fig. 4 (b)). The action is repeated until the last joint is locked (Fig. 4 (c)-(d)). At last, the shape of the robotic grasper is similar to the object. We can decide the state of all the joints as needed. For example, if only the first joint is unlocked, the robotic grasper will form a full-actuated hand (Fig. 4 (e)).

When grasping this kind of complex-shaped object, if all the joints are unlocked. And the shape of the finger would be like that in Fig. 4 (f), which is caused by the force between each joint. Compared with the state formed based on the ARM as shown in Fig. 4 (e), the contact area of this state is smaller, leading to weak grasping effect.

This control method is suitable for most of the complex objects. However, if the object is too complex that the modules cannot contact the object one by one during the process, this control method cannot ensure that the shape of the robotic grasper is the same as the shape of the object.

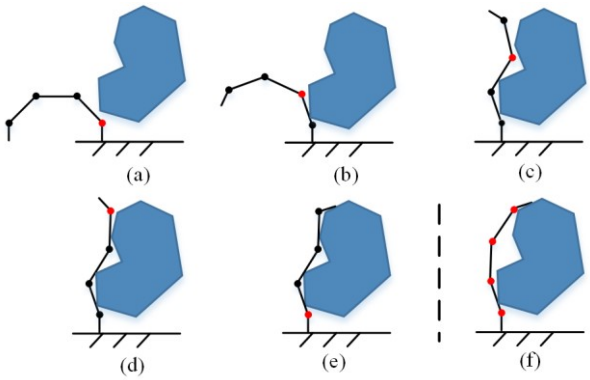

Fig. 4. The shape variation process of one finger based on the ARM; (a)-(e) show the states of grasping based on the ARM; (f) shows the state of grasping directly with all the joints unlock; Black joints represent locked joints and red joints represent unlocked joints

V. Experimental Validation

It is a challenge to characterize the robotic grasper because of its different performance when grasping objects. We design three preliminary experiments. The first experiment is to obtain the maximum grasping force of the robotic grasper. The second experiment is to grasp some typical common items in daily life, through pre-changing the number of the modules and presetting the shape of the robotic grasper, aiming to verify that the robotic grasper can grasp diverse objects. The third experiment is to verify the feasibility of the ARM we have proposed by changing the shape of the robotic grasper automatically during the process of the grasping motion.

A. Experimental Setup

We started from a simple configuration of robotic grasper with two fingers as the initial prototype in the experiments (Fig. 5). Each finger has four modules at the beginning and is driven by a Maxon brush motor (RE 25, Maxon Motor AG, Sachseln, Switzerland). Bowden-cables (Flat coil: external diameter: 4 mm, inner diameter: 1.5 mm; Cable: external diameter: 1 mm, Meiyue Metal CO., LTD., Dongguan, China) are used to link the robotic grasper and the motors. The clutches (BJ-2.6, SHINKO ELECTRIC CO., LTD, Nagano-shi, Japan) are used to lock or unlock the joints. The Hall current sensor (HCS-LTS, Zhitong Chuangan Technology CO., LTD., Wenzhou, China) is used to measure the motor current. The motors are controlled by a SimLab board (Zeltom LLC, Belleville, America), which can control the motion of the motors, the states of the clutches and collect data such as the angle, velocity and current of the motors in real-time. The amplifying board is used to control the clutches. The adjusting block is used to adjust the length of the cable inside the finger when the number of the modules is changed. The force sensor (HEX-E, Force capacity: 200 N, Resolution: 0.8 N, Optoforce Ltd., Hungary) is used to test the maximum grasping force of the robotic grasper.

1083-4435 (c) 2017 IEEE. Personal use is permitted, but republication/redistribution requires IEEE permission. See http://www.ieee.org/publications_standards/publications/rights/index.html for more information.

This article has been accepted for publication in a future issue of this journal, but has not been fully edited. Content may change prior to final publication. Citation information: DOI 10.1109/TMECH.2017.2765081, IEEE/ASME Transactions on Mechatronics

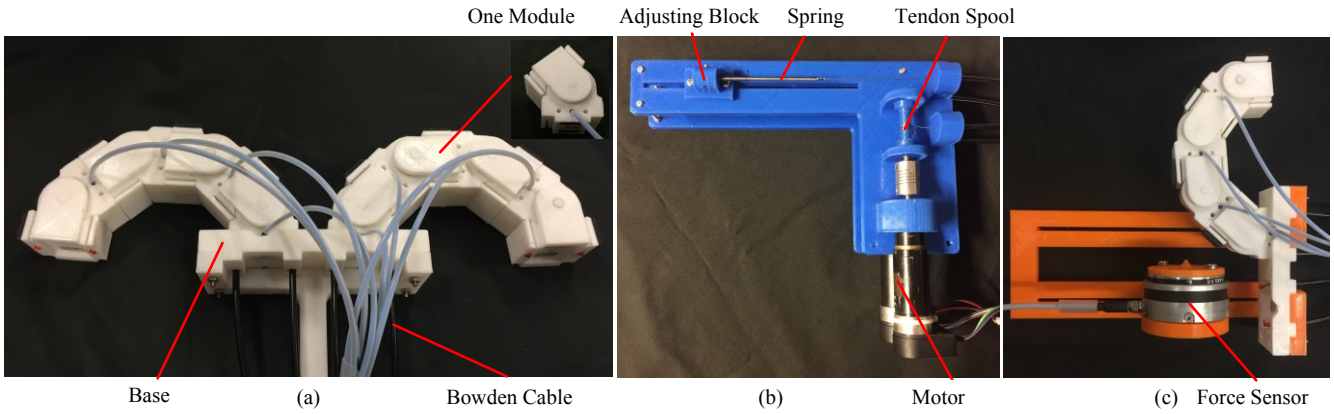

Fig. 5. Prototype of the robotic grasper: (a) the main body of the robotic grasper; (b) the Bowden-cable based driven system: (c) the platform for maximum grasping force test

B. *Maximum Grasping Force Test*

When the robotic grasper forms an under-actuated structure, the grasping force with multiple force acting points is related to the shape of the object. This creates difficulties for evaluating the grasping strength performance of the robotic grasper. As a result, we test the maximum grasping force when the robotic grasper forms a fully actuated structure.

As shown in Fig. 5, the force sensor fixed on an adjustable supporting structure is put in front of the finger. The finger is formed by finger modules with the number ranging from one to four. The first joint is unlocked and the other joints are locked. Then the finger is controlled to move. When the current achieves the rated current of the motor (1.67 A), the motion of the finger is stopped. The maximum grasping force acting on the force sensor vertically is shown in Table I.

TABLE I
RESULTS OF THE MAXIMUM GRASPING FORCE TEST

Number of finger modules	Maximum grasping force (N)
1	26
2	11
3	7
4	6

The maximum grasping force of the robotic grasper with one finger module is 26 N, and decreases to 6 N when the number of the finger modules increases to four. The maximum force is enough for the commonly used objects in daily life though it can be increased by using more powerful motors if needed. The maximum grasping force is not the only factor that determine the grasping performance. The shape of the robotic grasper also plays an important role, which will be tested in the second experiment.

C. *Grasping Ability Tests*

With the purpose of testing the grasping ability of the robotic grasper, we chose some common and typical daily necessities with different shapes, sizes, weights, surface conditions and stiffness for experiments. The robotic grasper is formed to different lengths by changing the number of the modules and different shapes by pre-setting the activity of the joints. The specific information is shown in Table II.

TABLE II
THE INFORMATION OF THE OBJECTS AND THE ROBOTIC GRASPER IN FIG. 6

Subfigure	Items	DOF of each finger	Features	Number of modules	Locked joints	Initial angles of the locked joints
a	Bottle filled with water	3	Round and heavy (Weight: 1.5 kg)	3	-	-
b	Strip-type bread	1	Long (Length: 205 mm) and soft	4	Second Third Fourth	0° 0° 0°
c	Coin	1	Small and flat (Thickness: 2.3mm)	2	First	0°
d	Grape*	1/2	Ductile and irregular shape	3	First Third	$-45°$ 45°
e	Succulent	2	Soft and irregular shape	4	First Fourth	$-45°$ $-45°$
f	Magnet with iron products	3	Complex surface shape and incompact	4	First	$-45°$
g	Egg	2	Fragile and smooth surface	3	First	0°
h	Durian	3	Heavy (Weight: 2.8 kg), spiny, large (Diameter: 193 mm) and complex surface shape	4	First	$-45°$

* The first joint is unlocked after two seconds from started

The position motion signal of the grasper is given in PC to control the grasping action. When the motor current achieves

1083-4435 (c) 2017 IEEE. Personal use is permitted, but republication/redistribution requires IEEE permission. See http://www.ieee.org/publications_standards/publications/rights/index.html for more information.

This article has been accepted for publication in a future issue of this journal, but has not been fully edited. Content may change prior to final publication. Citation information: DOI 10.1109/TMECH.2017.2765081, IEEE/ASME Transactions on Mechatronics

the preset values, the motion of the grasper is stopped. From the results in Fig. 6, the robotic grasper can successfully grasp objects with round, long, flat, small or irregular shapes, heavy or light weights, complex or smooth surfaces, and fragile, hard or soft surfaces. It is verified that the proposed robotic hand can grasp numerous irregular unknown objects.

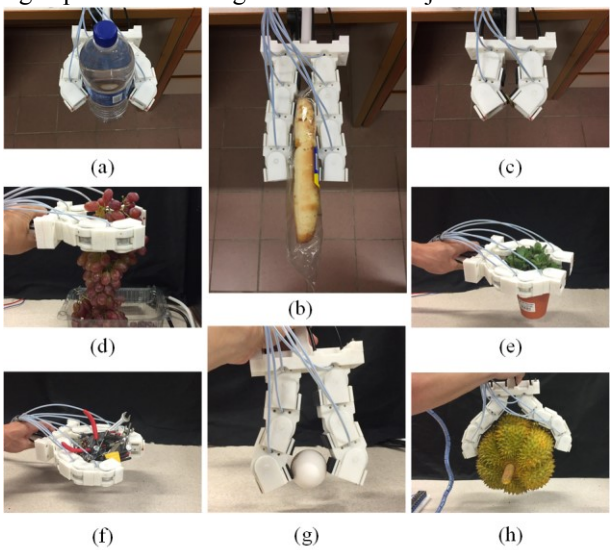

Fig. 6. Results of grasping diverse objects (details in Table I)

Clutches play a critical role in grasping performance via pre-changing the shape and DOF of the robotic grasper. The robotic finger would be either fully actuated when each finger only has one module or under-actuated for more than one modules without clutches:

- Fully actuated robotic grasper: Each finger has only one DOF and is not adaptive to the object. The lack of contact area may lead to failure when grasping round and smooth surface objects (e.g., bottle filled with water and egg), soft and irregular objects (e.g., succulent), large objects (e.g., durian) and incompact objects (e.g., the magnet with iron products).
- Under-actuated robotic grasper: When grasping an object, the robotic grasper may form the shape as shown in Fig. 4 (f). Long object (e.g., strip-type bread) is not easy to be grasped because the grasper may have a point contact with the objects. Besides, when grasping small objects (e.g., coin), the terminal pose is not easy to control.

In the process of grasping, clutches also make it possible to change the shape of the robotic grasper, e.g. when grasping the grape, the first joint is locked at the beginning to provide enough opening angle, and after two seconds, it is unlocked to adapt to the shape of the object better.

The robotic grasper with more numerous finger modules each finger can form complex shape to contact with objects better and are fit for grasping long or large objects (strip-type bread and durian), while the one with fewer modules has advantages in grasping small objects (coin). If the robotic grasper has too many modules, the drawbacks are obvious: a) the length of the finger would be too long to grasp small objects; b) the weight would increase, leading to the accuracy and stability not easy to control; c) the terminal cannot provide enough grasping force as shown in the maximum grasping force test. From the results of the experiments, 2-4 modules each finger can meet the requirements of grasping the common objects in daily life.

The payload capacity is determined by multiple factors: a) the power of the actuators; b) the strength of the mechanism; c) the grasping mode and d) the properties of the objects. In other words, the robotic grasper may grasp a cup with a certain weight successfully. However, it probably cannot grasp a bunch of grapes with the same weight. As for the robotic grasper, the weights of the base and the finger module are 0.08 kg and 0.05 kg, respectively. The total weight is determined by the number of the finger modules. As a result, it is difficult to obtain a constant ratio of payload to weight. Accordingly, we take the bottle filled with water and durian in the experiments as examples as their weights are heavier than others. The ratios of payload to weight are 4 and 2.8, respectively.

D. Self-adapted Shape Control Experiment

As known in Section IV, when the robotic grasper contacts the object, the states of the joints need to be changed., Due to the positive correlation between F_a and I_m, whether the robotic grasper contacts the object or not can be determined by detecting I_m. First, the maximum values of I_m are obtained which may appear when rotating each joint without load. Then I_m^{max} is set which is higher than the maximum values of I_m as the threshold values. During the process of grasping, if $I_m > I_m^{max}$, it can be considered that the robotic grasper contacts the object.

One finger is taken as an example. The values of I_m in the absence of load are shown in Fig. 7. The maximum current values for each joint are 0.72 A, 0.74 A, 1.19 A and 1.11 A, respectively. The threshold values are determined by combining a) judging whether the robotic grasper contacts the object or not as mentioned above, and the first to fourth threshold values should be higher than the corresponding maximum current values for the first to fourth joints in Fig. 7 respectively; b) for programming convenience, the latter value should be higher than the previous one to ensure the states of the joints can be changed one by one; c) the threshold values should be no higher than the rated currents of the motors used. Hence, I_m^{max} is set as 0.8 A, 1.0 A, 1.3 A and 1.5 A respectively. The first three threshold values are the references of converting the states of clutches and the last threshold value is used to determine the grasp force.

1083-4435 (c) 2017 IEEE. Personal use is permitted, but republication/redistribution requires IEEE permission. See http://www.ieee.org/publications_standards/publications/rights/index.html for more information.

This article has been accepted for publication in a future issue of this journal, but has not been fully edited. Content may change prior to final publication. Citation information: DOI 10.1109/TMECH.2017.2765081, IEEE/ASME Transactions on Mechatronics

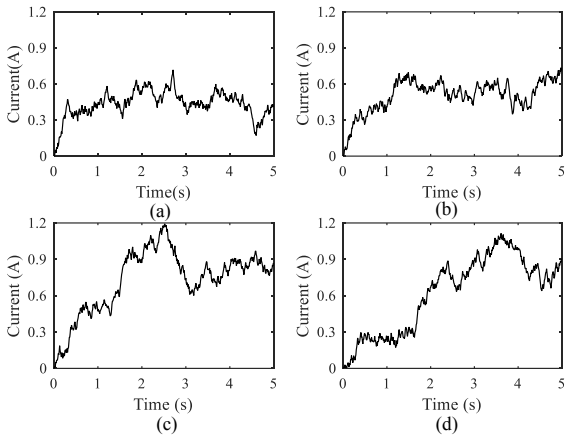

Fig. 7. Current of the motor when controlling the motion of the robotic grasper without load. (a)-(d) is corresponding to the first to fourth joints

The cup is the grasping object in this experiment. The procedure is as follows: Firstly, the initial pose of the robotic grasper is set and the object is positioned in front of the robotic grasper. Then the fingers are driven to grasp the object. When $I_m > I_m^{max}$, each joint is automatically locked by the related clutch. The process of operation is shown in Fig. 8. In Fig. 8 (a), the first joint is unlocked while the others are locked. The grasper begins to grasp. The Fig. 8 (b)-(d) shows the process of the grasping motion. The second to the fourth joints begin to be unlocked successively and the others are locked. After that, as shown in Fig. 8 (e), the grasping is finished. The shape of the robotic grasper is conformable to the cup.

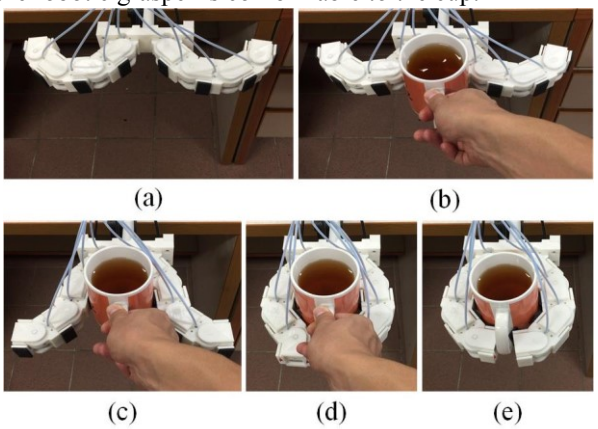

Fig. 8. The process of grasping cup based on the ARM

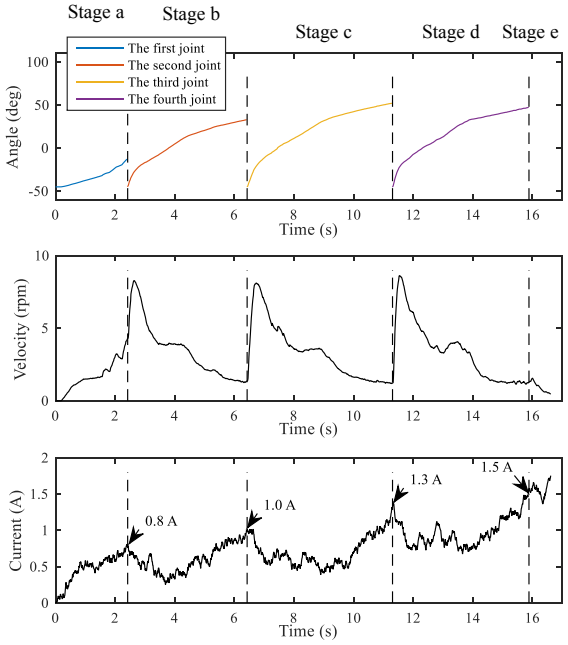

Fig. 9. The angles and velocities of joints and the current of one motor driving the left finger in Fig. 8. Each sub-figure is divided into five stages by dotted lines, which correspond Fig. 8 (a)-(e)

The shape of the robotic grasper can be seen from Fig. 8. However, the role that the clutches play and how the clutches affect the motion of the robotic grasper are not clear. As a result, the angle and velocity of the joints, and the current of the motors during the grasping process are measured as shown in Fig. 9. The angles, velocities and the currents of the motors are obtained by Simlab broad. The angles and velocities of the joints are calculated through the kinematics mentioned in Section III.

As shown in Fig. 8 and Fig. 9, the grasping process is divided into 5 stages, caused by changing the states of clutches. The first joint rotates in the first stage, and so do the other three joints. In the fifth stage, the grasper keeps holding the object.

Fig. 9 (a) shows the angles of the four joints in the stages of (a) to (d) in Fig. 8. In stage e, the shape of the robotic grasp keeps unchanged. They appear consistent with the actual situation as shown in Fig. 8, e.g., the angle of the first joint is smaller than others since the shape of the object is circular. Fig. 9 (b) shows that the velocity is periodic. At each stage, the velocity first increases obviously and then decreases. On the contrary, in Fig. 9 (c), the current first decreases and then increases. This is because in each early stage, there is no counter force from the object, and then the robotic grasper begins to contact the object, leading to the gradually larger counter force. From an overall perspective, the trend of the current is going up. The reason is that the spring force is increased when grasping.

VI. Conclusion and Future Work

In this paper, a cable driven robotic grasper with modular, reconfigurable and flexible joints and is proposed and detailed

1083-4435 (c) 2017 IEEE. Personal use is permitted, but republication/redistribution requires IEEE permission. See http://www.ieee.org/publications_standards/publications/rights/index.html for more information.

This article has been accepted for publication in a future issue of this journal, but has not been fully edited. Content may change prior to final publication. Citation information: DOI 10.1109/TMECH.2017.2765081, IEEE/ASME Transactions on Mechatronics

design features are described. The robotic grasper integrates the advantages of a full actuation and under-actuation and is designed to grasp diverse daily necessities with complex shapes, especially in unstructured environment, using a simple control scheme.

One of the main features of the robotic grasper is the Lego-like modular structure that improves the easiness for module assembly, offline or online. The modules connected by magnets can be manually installed or removed, to the extent that the length of the robotic grasper can be adjusted. The second feature is the reconfigurable flexible joints. The shape and the DOF of the robotic grasper can be changed by locking or unlocking the clutches in the joints and the locked joints can reduce the continuous current of motors. This clutch-based design efficiently improves the grasping ability through a simple mechanism. The Bowden-cable driving method can reduce the volume and weight of the body of the robotic grasper, making it easy to be mounted on a robotic arm.

The kinematics, workspace and contact forces are analyzed. The range of the workspace is determined by the number of the modules and the states of the joints. Accordingly, the ARM during the process of operation is proposed. This method allows the shape of the robotic grasper to adapt to the object during the operation. The maximum grasping force is measured and analyzed. The ability of grasping diverse objects and the effectiveness of the ARM are verified.

Future work includes more accurate contact force estimation and analysis in a complex environment, as well as a more effective intelligent control method for improving its grasping ability.

ACKNOWLEDGEMENTS

This work is supported by Singapore Millennium Foundation under Grant R-397-000-201-592 and Office of Naval Research Global under Grant ONRG-NICOP-N62909-15-1-2029 awarded to Dr. Hongliang Ren. We would like to thank Ifetayo-Haleema Miller, Dr. Da Sun and Dr. Ning Tan for their enthusiastic help.

REFERENCES

[1] A. M. Dollar and R. D. Howe, “Joint coupling design of underactuated hands for unstructured environments," *Int. J. Robot. Res.,* vol. 30, no. 9, pp. 1157-1169, 2011.

[2] R. Diankov and J. Kuffner, "OpenRAVE: A Planning Architecture for Autonomous Robotics," *Pittsburgh, PA, Tech. Rep. CMU-RI-TR-08-34*, July. 2008.

[3] V. Lippiello, F. Ruggiero, B. Siciliano, and L. Villani, "Visual Grasp Planning for Unknown Objects Using a Multifingered Robotic Hand," *IEEE/ASME Trans. Mechatronics,* vol. 18, no. 3, pp. 1050-1059, 2013.

[4] J. K. Salisbury and J. J. Craig, "Articulated Hands: Force Control and Kinematic Issues," *Int. J. Robot. Res.,* vol. 1, no. 1, pp. 4-17, 1982.

[5] Jacobsen, S.C., et al., "The Utah/MIT dextrous hand work in progress, " *Int. J. Robot. Res.,* vol. 3, no. 4, pp. 21-50, 1984.

[6] Grebenstein, M., Chalon, M., Friedl, W., Haddadin, S., Wimböck, T., Hirzinger, G. and Siegwart, R., "The hand of the DLR Hand Arm System: Designed for interaction," *Int. J. Robot. Res.,* vol. 31, no. 13, pp. 1531-1555, 2012.

[7] A. M. Dollar and R. D. Howe, "The Highly Adaptive SDM Hand: Design and Performance Evaluation," *Int. J. Robot. Res.,* vol. 29, no. 5, pp. 585-597, 2010.

[8] L. U. Odhner, L. P. Jentoft, M. R. Claffee, N. Corson, Y. Tenzer, R. R. Ma, M. Buehler, R. Kohout, R. D. Howe, and A. M. Dollar, "A compliant, underactuated hand for robust manipulation," *Int. J. Robot. Res.,* vol. 33, no. 5, pp. 736-752, 2014.

[9] N. Tan and H. Ren, "Positioning evaluation of tendon-driven flexible manipulators based on interval analysis," *Electron. Lett,* vol. 52, no. 21, pp. 1748-1749, 2016.

[10] N. Dechev, W. L. Cleghorn and S. Naumann, "Multiple finger, passive adaptive grasp prosthetic hand," *Mech. Mach. Theory,* vol. 36, no. 10, pp. 1157-1173, 2001.

[11] D. L. Akin, C. R. Carignan and A. W. Foster, "Development of a four-fingered dexterous robot end effector for Space operations," in *Proc. IEEE Int. Conf. Robot. Autom,* Washington DC, USA, 2002, pp. 2302-2308.

[12] H. Wang, C. Wang, W. Chen, X. Liang and Y. Liu, "Three-Dimensional Dynamics for Cable-Driven Soft Manipulator, " *IEEE/ASME Trans. Mechatronics,* vol. 22, no. 01, pp. 18-28, 2017.

[13] N. Dechev, W. L. Cleghorn and S. Naumann, "Multiple finger, passive adaptive grasp prosthetic hand," *Mech. Mach. Theory,* vol. 36, no. 10, pp. 1157-1173, 2001.

[14] Belzile, B. and L. Birglen, "Stiffness Analysis of Underactuated Fingers and its Application to Proprioceptive Tactile Sensing, " *IEEE/ASME Trans. Mechatronics,* vol. 21, no. 6, pp. 2672-2681, 2016.

[15] L. P. Jentoft, W. Qian and R. D. Howe, "Limits to compliance and the role of tactile sensing in grasping," in *Proc. IEEE Int. Conf. Robot. Autom,* Hongkong, China, 2014, pp. 6394-6399.

[16] T. Takaki and T. Omata, "100g-100N finger joint with load-sensitive continuously variable transmission," in *Proc. IEEE Int. Conf. Robot. Autom, ,* Orlando, Florida, USA, 2006, pp. 976-981.

[17] D. M. Aukes, B. Heyneman, J. Ulmen, H. Stuart, M. R. Cutkosky, S. Kim, P. Garcia and A. Edsinger, "Design and testing of a selectively compliant underactuated hand," *Int. J. Robot. Res.,* vol. 33, no. 5, pp. 721-735, 2014.

[18] H. Wang, B. Yang, Y. Liu, W. Chen, X. Liang, R. Pfeifer, "Visual servoing of soft robot manipulator in constrained environments with an adaptive controller, " *IEEE/ASME Trans. Mechatronics*, vol. 21, no. 1, pp. 41-50, 2017.

[19] Z. Li, H. Ren, P. W. Y. Chiu, R. Du, H. Yu, "A novel constrained wire-driven flexible mechanism and its kinematic analysis," *Mech. Mach. Theory*, vol. 21, pp. 59-75, 2016.

[20] Z. Li, L. Wu and H. Ren, "Kinematic comparison of surgical tendon-driven manipulators and concentric tube manipulators," *Mech. Mach. Theory*, vol. 107, pp. 148-165, 2017.

[21] R. Vinet, Y. Lozac'H, N. Beaudry, and G. Drouin, "Design methodology for a multifunctional hand prosthesis," *J. Rehabil. Res. Dev.,* vol. 32, no. 4, pp. 316-24, 1995.

[22] J. L. Pons, E. Rocon, R. Ceres, D. Reynaerts, B. Saro, S. Levin and W. Van Moorleghem, "The MANUS-HAND Dextrous Robotics Upper Limb Prosthesis: Mechanical and Manipulation Aspects," *Auton. Robots,* vol. 16, no. 2, pp. 143-163, 2004.

[23] H. Kawasaki, T. Komatsu and K. Uchiyama, "Dexterous anthropomorphic robot hand with distributed tactile sensor: Gifu hand II," *IEEE/ASME Trans. Mechatronics,* vol. 7, no. 3, pp. 296-303, 2002.

[24] J. Ueda, M. Kondo and T. Ogasawara, "The multifingered NAIST hand system for robot in-hand manipulation," *Mech. Mach. Theory,* vol. 45, no. 2, pp. 224-238, 2010.

[25] A. Namiki, M. Ishikawa, Y. Imai, and M. Kaneko, "Development of a High-speed Multifingered Hand System," in *Proc. IEEE Int. Conf. Robot. Autom,* Taibei, China, *2003.*

[26] M. C. Carrozza, C. Suppo, F. Sebastiani, B. Massa, F. Vecchi, R. Lazzarini, M.R. Cutkosky, P. Dario, "The SPRING Hand: Development of a Self-Adaptive Prosthesis for Restoring Natural Grasping," *Auton. Robots*, vol. 16, no. 2, pp. 125-141, 2004.

[27] S. Shirafuji, S. Ikemoto and K. Hosoda, "Development of a tendon-driven robotic finger for an anthropomorphic robotic hand," *Int. J. Robot. Res.,* vol. 33, no. 5, pp. 677-693, 2014.

1083-4435 (c) 2017 IEEE. Personal use is permitted, but republication/redistribution requires IEEE permission. See http://www.ieee.org/publications_standards/publications/rights/index.html for more information.